LAWRENCE
LIVERMORE
NATIONAL
LABORATORY

UCRL-JRNL-207191

Hohlraum-driven ignition-like double-shell implosions on the Omega laser facility

P. Amendt, H. F. Robey, H. S. Park, R. E. Tipton, R. E. Turner, J. L. Milovich, M. Bono, R. Hibbard, H. Louis, R. Wallace

October 12, 2004

Physical Review Letters

Hohlraum-driven ignition-like double-shell implosions on the Omega laser facility

Peter A. Amendt, Harry F. Robey, H.-S. Park, R.E. Tipton, R.E. Turner, J.L. Milovich, M. Bono, R. Hibbard, H. Louis, R. Wallace
Lawrence Livermore National Laboratory, Livermore, California 94550

V. Yu. Glebov
Laboratory for Laser Energetics, U. of Rochester

High-convergence ignition-like double-shell implosion experiments have been performed on the Omega laser facility [T.R. Boehly *et al*., Opt. Commun. **133**, 495 (1997)] using cylindrical gold hohlraums with 40 drive beams. Repeatable, dominant primary (2.45 MeV) neutron production from the mix-susceptible compressional phase of a double-shell implosion, using fall-line design optimization and exacting fabrication standards, is experimentally inferred from time-resolved core x-ray imaging. Effective control of fuel-pusher mix during final compression is essential for achieving noncryogenic ignition with double-shell targets on the National Ignition Facility [Paisner *et al*., Laser Focus World **30**, 75 (1994)].

PACS numbers: 52.40.Nk, 52.50.Jm, 52.58.Ns

The goal of inertial confinement fusion is to implode a low-Z capsule filled with deuterium-tritium (DT) to a sufficient density and temperature for achieving thermonuclear ignition and energy gain [1]. In the single-shell indirect-drive option, a capsule is placed at the center of a high-Z radiation enclosure (or hohlraum) which converts absorbed laser rays into x rays that ablate the capsule and drive an implosion. This current mainline ignition option requires cryogenic filling of the capsule (using an *in situ* fill-tube) near the triple point of deuterium (18.3°K) and careful shock sequencing to maintain the fuel on a low enough adiabat for achieving thermonuclear burn and high gain (>10) [2]. The required laser drive for pre-forming the DT-ice pusher to sufficient density ($\approx 10^3$g/cc) uses a high contrast pulse-shape (50-to-1 peak-to-foot), delivering high power at late time when the hohlraum has filled with plasma.Such a hohlraum environment may lead to harmful laser backscatter from parametric instabilities.

A complementary approach to demonstrating ignition utilizes noncryogenic double-shell targets where a dense, high-Z, seamless inner shell provides inertial confinement and radiation trapping. With less need for careful shock-timing, the requirements on the laser pulse-shape are less strict, allowing the option of a more benign power history and the prospect of reduced laser backscatter. An added property of double shells is that the mode of thermonuclear burn is via volume ignition [3] instead of (10 keV) hot-spot ignition [2]. Although the gain (of 2 to 4) is comparatively low with current double-shell target designs [4,5] for the National Ignition Facility (NIF) [6], the lower threshold ignition temperature of ≈4 keV makes ignition easier by relaxing the requirements on implosion symmetry. However, the main challenge with double-shell ignition is the required control of mix of high-Z pusher material and DT fuel to low levels.

The concept of double-shell ignition has been tested over the past ten years with experiments on the Nova [7] and Omega [8] laser facilities using low-Z inner shells to accommodate the limited available energy. A standard metric of implosion performance is the ratio of the measured primary neutron yield [$D+D \rightarrow n(2.45\ \text{MeV})+He^3(0.82\ \text{MeV})$] to the calculated "clean" yield, i.e., no mix, or "YoC" [9]. All-glass inner-shell double-shell experiments have consistently given YoCs of a few percent at most, thereby challenging our notions of double-shell behavior. Recently, double-shell experiments were fielded on the Omega laser with hybrid glass/plastic inner shells that gave YoCs closer to unity [10]. A key feature of these experiments is that preheat M-band x-ray radiation (2-5 keV) from the laser-irradiated gold hohlraum walls causes the inner shell to expand appreciably before arrival of the ablatively-driven first shock, resulting in only premature "first-shock" [11] neutron burn. However, a key ingredient of ignition-like behavior is the participation of a second shock originating from the rarefaction fan in the outer shell [5]. This fan reflects off the ablation front in the outer shell, becoming a compressional wave that steepens into a second shock upon inner-shell transit. An ignition-like "two-shock" double-shell implosion is characterized by weak first-shock neutron burn (<1%), followed by shock coalescence in the fuel and the associated compression or stagnation neutron burn. A challenge of double-shell ignition research is to demonstrate control of debilitating fuel-pusher mix so that the vast majority of neutrons are produced during compression – a prerequisite for achieving ignition [12]. In this Letter we demonstrate repeatable ignition-like double-shell behavior with compression-dominated neutron yields as inferred from time-resolved hard x-ray core emission. Moreover, we show that the double-shell performance is comparable to the highest performing hohlraum-driven single-shell implosions to date on Omega [13] – and at higher fuel convergence [14]. This result was made possible by exacting target fabrication, careful laser power control, and physical design criteria geared to reducing the effects of fuel-pusher mix.

The Omega indirect-drive double-shell experimental configuration is shown in Fig. 1. Three cones with 5, 5, and 10 beams, respectively, enter each end of the gold hohlraum through a 75% (of the hohlraum diameter) laser-entrance hole (LEH) at three distinct angles to the axis of symmetry: θ=21.4°, 42°

and 58.9°. The 0.351μm wavelength laser energy (<16 kJ) is absorbed in the gold hohlraum wall and re-radiated as a quasi-Planckian spectrum of x rays with a hard component at 2-5 keV [*n*=4→3]. The thermal x rays (<1 keV) are absorbed in the outer shell which consists of polystyrene (CH) and 2% [at.] bromine doping for x-ray preheat control in the all-CH inner shell. The ablating (and converging) outer shell then collides (mostly inelastically) with the inner shell, compressing the encapsulated DD fuel to thermonuclear conditions (> 1 keV).

Two design considerations were used in this double-shell implosion campaign. First, the goal was to have the compression stage of (clean) neutron production largely dominate the earlier shock-flash neutron burst in order to mimic the behavior of a proposed igniting double-shell on the NIF [5]. The second (and related) goal is the control of mix between the fuel and pusher (induced by Rayleigh-Taylor instability growth) to ensure appreciable compression neutron production. A useful figure-of-merit for controlling mix is the "fall-line" delay to the origin [5]. Physically, the fall-line is the trajectory of free-falling interfacial material after deceleration onset. From causality considerations little, if any, pusher material is expected ahead of the fall-line trajectory, so that an arranged large delay in the fall-line relative to the instant of peak neutron burn gives added margin to mix.

The double-shell target dimensions were specified to meet these two design goals [See Fig. 1], and strict fabrication requirements [15] were applied to ensure repeatable target performance. Micro-machined carbonized-resorcinal-formaldehyde foam hemispherical inserts of density 50mg/cc were used to support the inner shell and meet the shell concentricity specification (<5μm). This foam material was chosen because of its favorable machining properties and inherently small pore size (<100nm) for added margin to the seeding of hydrodynamic instability growth following shell collision [16]. The outer shell consisted of two hemispherical shells with a machined epoxy-filled step joint to ensure complete (4π steradian) x-ray shielding of the inner shell. The assembled double-shell target was then sandwiched between two ≈600-1000Å thick Formvar® tents for mounting at the hohlraum center.

The laser pulse-shape was chosen to maintain a nominal hohlraum drive temperature of ≈185 eV up to 2.5ns [See Fig. 2]. This temperature was monitored with an array of calibrated x-ray diodes ("Dante" [17]) viewing through the LEH at 37° from the symmetry axis. Figure 2 shows that the comparison between measured and postprocessed two-dimensional (2D) radiation-hydrodynamics simulations is well within the measurement uncertainties. Full-aperture laser backscatter measurements on the outer two cones

(42°, 58.9°) show negligible levels (<200J total), as expected for this pulse-shape. The highest energy channels of Dante provides a temporal record of 2-5 keV radiation exiting the LEH. Figure 3 compares the measured and postprocessed M-band fraction, showing agreement at late time but a significant difference up to 1.5ns. To correct for this difference, the nominal non-local thermodynamic equilibrium calculation with shell-averaged Au opacities (XSN [18]) made use of time-dependent Au emissivity opacity multipliers (<3×) above 2 keV. As a consistency check, these multipliers were then applied to modeling a dedicated diagnostic target for measuring the M-band strength at hohlraum center. This double-shell diagnostic target was specifically designed to implode a CH-tamped glass inner shell with non-thermal (>1 keV) x rays alone by delaying shell collision with an oversized outer shell. The trajectory of the imploding glass shell was inferred from 60ps gated backlit images. Figure 4 shows the measured and calculated trajectory of the inner shell transmission minimum with and without enhanced M-band x-ray emission. This independent (and integrated) measure of the M-band fraction confirms the high level of early time preheat seen with Dante and supports our phenomenological preheat analysis.

Figures 2-4 collectively argue for a consistent understanding of the level of thermal and M-band x-ray drive in the experiment. The focus on M-band fraction is derived from the expected high sensitivity of an Omega-scale double-shell implosion to x-ray preheat. With the limited energy available on Omega for the prescribed pulse-shape (See Fig. 2), the inner shell must be thin enough to reach a sufficiently high implosion velocity - but not so thin that feed-through of hydrodynamic instability leads to shell breakup. For our chosen inner shells, the optical depth of a 2 keV photon is less than unity and leads to volumetric expansion and reduced hydrodynamic efficiency. Figure 5(a) shows the observed neutron yield compared to the simulated first-shock yield for all six double-shell implosions. Of these targets, the first five met all fabrication specifications. The first used a 13μm thick inner shell and 0.1atm Ar doping in the fuel for core imaging [See Fig. 1], while the next four targets used a nominally thicker inner shell (17μm) to provide added margin to potential shell breakup from perturbation feed-through. For each of these targets, the neutron yield far exceeds the shock-flash yield as designed. The final target (#6) in Fig. 5(a) had a large (≈4 _m) joint gap as well as an azimuthal machining defect in the outer shell which was patched with a nearly density-matched epoxy and re-machined. The measured yield of this "control" capsule is just above the level from first-shock, suggesting that strong mixing compromised the compression phase of the implosion.

Figure 5(b) compares the performance of the first five double-shells with the Omega cylindrical hohlraum implosion database. The former single-shell targets [13] refer to 1% Ge-doped CH single-shell implosions driven by a medium contrast ratio (5-to-1) pulse-shape. Three surrogate single-shell capsules were fielded along with the double shells to assess hohlraum radiation symmetry and to provide a direct comparison in performance. The YoC_{2D} metric refers to the inclusion of calculable 2D intrinsic hohlraum radiation asymmetry effects on the simulated yield and a ≈3% systematic left-right laser power imbalance. The fall-line parameter $\Delta\tau$ is defined as the peak burn time minus the fall-line time, normalized to the FWHM burn width. As expected, the double-shell targets show more sensitivity to M-band preheat than the single-shell surrogates [19], cf. open and solid symbols in Fig. 5(b). Despite the effect of enhanced M-band preheat on double-shell performance (≈2× reduction in simulated DD neutron yield), the calculated (clean) compression neutron yield fraction remains above 99%. With M-band enhancement to match the Dante measurement, both surrogate single shells and the double-shell targets follow a slow decline in neutron performance with increasing fall-line parameter. Furthermore, the performance of the double-shell implosions is comparable to the highest convergence (≈20) single-shell capsules (5atm DD fill) to date, attaining a YoC_{2D} up to 35% for a calculated clean convergence≈30.

Gated hard (3-5 keV continuum) x-ray argon self-emission imaging of the imploded fuel core was successfully used to infer dominant compression neutron burn and adequate core symmetry. Figure 6 shows good agreement between the measured and predicted x-ray emission history for the double-shell target. Also shown is a comparison of the peak x-ray emission images of a surrogate and the double-shell target, showing reasonable symmetry of the double shell despite ≈50% higher fuel convergence. The origin of the core asymmetry is believed due to a combination of M-band hohlraum asymmetry and hydrodynamic jetting from the outer-shell seam. Both the timing history and image sizes are consistent with dominant compression neutron production and collectively argue for minimal shock-flash neutron burn as predicted.

In summary, repeatable ignition-like hohlraum-driven double-shell implosions were demonstrated for the first time on the Omega laser facility. High fractional compression neutron yields and implosion performance on par with high-convergence single-shell implosions were observed. The consistency in performance with the fall-line parameter for a variety of target types and fuel convergences provides validation of this metric as a mix-mitigation design tool for enabling double-shell ignition on the NIF.

This work was performed under the auspices of the U.S. Department of Energy by UC, Lawrence Livermore National Laboratory under Contract No. W-7405-Eng-48.

Figure Captions

Fig. 1: Three-dimensional rendering of hohlraum and Omega laser geometry. Hohlraum length (radius) is 2500 (800) μm; inner beams (red) cross symmetry axis at ±1850μm, intermediate beams (green) cross axis at 1400μm, and outer beams (blue) cross at 1200μm. Also shown is preshot radiograph of a double-shell implosion target with 2%-Br-doped CH outer shell (o.d.=550μm, i.d.=446μm) and CH inner shell (o.d.=244μm, i.d.=218μm) containing 50atm of DD and 0.1atm of argon dopant.

Fig. 2: Measured (open squares) and simulated (solid) Dante drive temperature versus time; delivered total laser power history (solid) and requested power history versus time (dashed). Dark shading denotes error bars.

Fig. 3: Measured (open squares) and simulated (dashed) Dante M-band flux fraction (2-5 keV) versus time. Also shown is phenomenologically-matched Dante M-band fraction using time-dependent Au emission opacity multipliers above 2 keV (solid). Dark shading denotes error bars.

Figs. 4: Measured (open squares) and simulated backlighter transmission minimum trajectories with (solid) and without (dashed) enhanced Au M-band fraction (2-5 keV) versus time [cf. Fig. 3] for early- and late-time M-band targets as schematically shown. Early-time target is backlit by Cr at 5.6 keV (in black) and late-time by Sc at 4.3 keV (in red); inner shell is web supported between two hemispherical butt-jointed outer shells.

Figs. 5(a-b): (a) Measured primary neutron yield (solid) and 2D simulated shock-flash neutron yield versus fielded double-shell implosion target; (b) observed-over-predicted primary neutron yield- versus dimensionless fall-line parameter $\Delta\tau$ (see text). In (b) former 1% Ge-doped CH single-shell data are shown in dark grey for indicated DD gas-fills; triangles denote single-shell surrogate capsules with (solid) and without (open) enhanced M-band radiation – squares indicate double-shell targets. Astericked targets had 0.1 atm argon dopant in fuel to facilitate x-ray (3-5 keV) core imaging; shown also is schematic of nominal surrogate capsule.

Fig. 6(a-b): Simulated and measured x-ray core self-emission history for double-shell target #1. Vertical line is measured neutron bang-time (NBT) [20]. Peak self-emission x-ray core image from imploded Ar-doped DD fuel for a surrogate single-shell capsule (top) and double-shell target (bottom) with 60 ps temporal resolution and 10 μm spatial resolution; solid white contour denotes 50% peak x-ray emission.

References

[1] J.D. Lindl, Inertial Confinement Fusion (*Springer-Verlag, New York, 1998*).

[2] S.W. Haan *et al.*, Phys. Plasmas **2**, 2480 (1995).

[3] H. Hora *et al.*, J. Plasma Phys. **60**(4), 743 (1998).

[4] D.B. Harris and W.S. Varnum, Bull Am. Phys. Soc. **41**, 1479 (1996).

[5] P. Amendt *et al.*, Phys. Plasmas **9**(5), 2221 (2002).

[6] J.A. Paisner *et al.*, Laser Focus World **30**, 75 (1994).

[7] E.M. Campbell, Laaser Part. Beams **9**, 209 (1991).

[8] T.R. Boehly *et al.*, Opt. Commun. **133**, 495 (1997).

[9] O.L. Landen *et al.*, Phys. Plasmas **5**, 768 (1998).

[10] W.S. Varnum *et al.*, Phys. Rev. Lett. **84**, 5153 (2000).

[11] R.D. Petrasso *et al.*, Phys. Rev. Lett. **90**, 095002 (2003).

[12] Compressional yields greater than shock-flash yields by at least a factor-of-100 are associated with significant charged particle (He^4) energy deposition in the fuel and onset of ignition.

[13] P. Amendt, R.E. Turner, and O.L. Landen, Phys. Rev. Lett. **89**, 165001 (2002).

[14] We follow convention [Ref. 1] and understand fuel convergence to mean the initial ablator radius divided by the imploded fuel radius.

[15] R.L. Hibbard *et al.*, Fusion Science Technology, to appear (2004).

[16] W. J. Garbett, private communication (2003).

[17] H.N. Kornblum, R.L. Kauffman, and J.A. Smith, Rev. Sci. Instrum. **57**, 2179 (1986).

[18] W.A. Lokke and W.H. Grasberger, “XSNQ-U, a non-LTE emission and absorption coefficient subroutine,” UCRL-52276, 1977; copies may be obtained from the National Technical Information Service, Springfield, VA 22161.

[19] The HEP5 single-shell database shows no comparable M-band anomaly principally because the forward-ramped pulse-shape that was used is associated with far less preheat at (computationally problematic) early time, cf. Fig. 3.

[20] C. Stoeckl *et al.*, Rev. Sci. Instrum. **73**, 3796 (2002).

Fig. 1

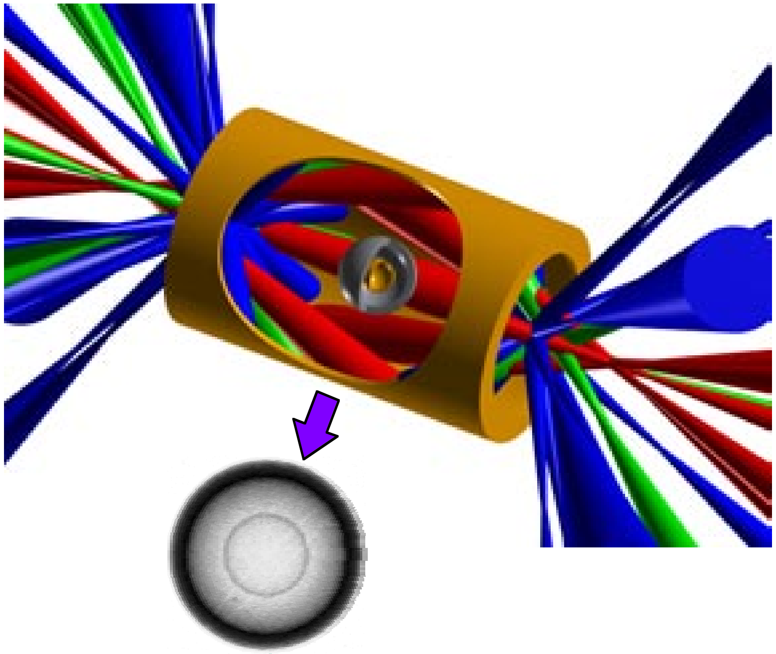

Fig. 2

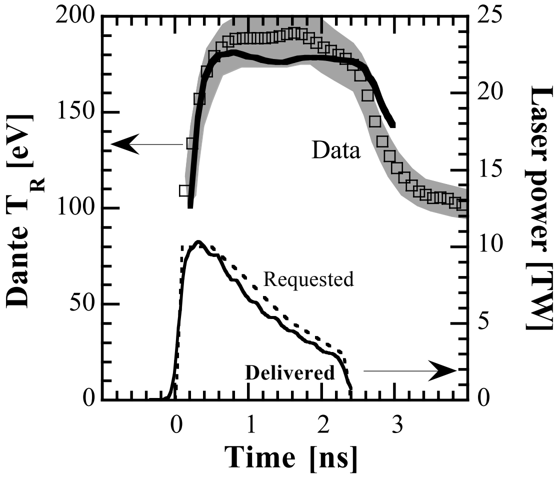
Dante T_R [eV]
Laser power [TW]
Time [ns]
Data
Requested
Delivered
0
50
100
150
200
0
5
10
15
20
25
0
1
2
3

Fig. 3

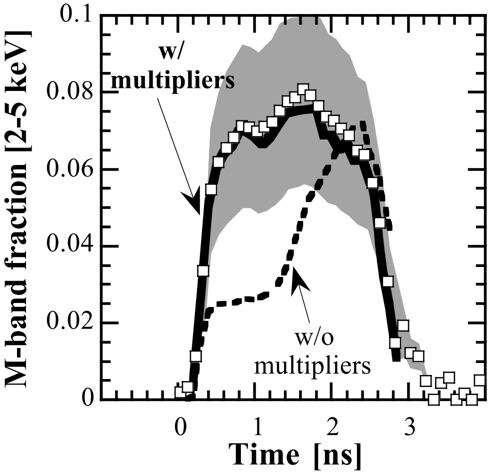
w/
multipliers
w/o
multipliers
M-band fraction [2-5 keV]
0
0.02
0.04
0.06
0.08
0.1
Time [ns]
0
1
2
3

Fig. 4

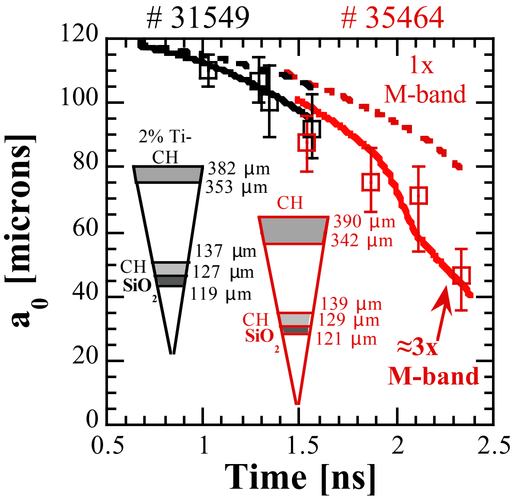

31549
35464
120
100
80
60
40
20
0
0.5
1
1.5
2
2.5
Time [ns]
a_0 [microns]
1x
M-band
≈3x
M-band
2% Ti-
CH
382 μm
353 μm
137 μm
CH
127 μm
SiO_2
119 μm
CH
390 μm
342 μm
139 μm
CH
129 μm
SiO_2
121 μm

Fig. 5(a)

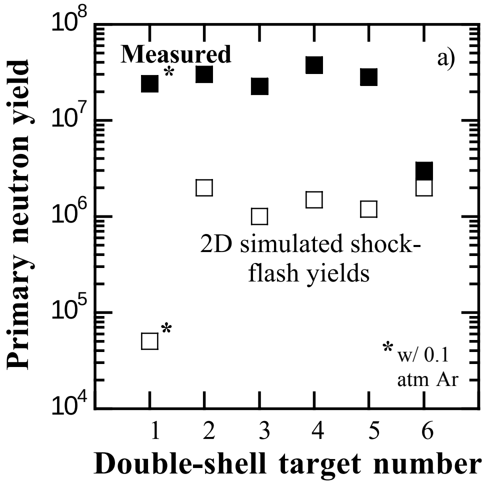

Measured
a)
*
2D simulated shock-flash yields
*
* w/ 0.1 atm Ar
10^8
10^7
10^6
10^5
10^4
Primary neutron yield
1
2
3
4
5
6
Double-shell target number

Fig. 5(b)

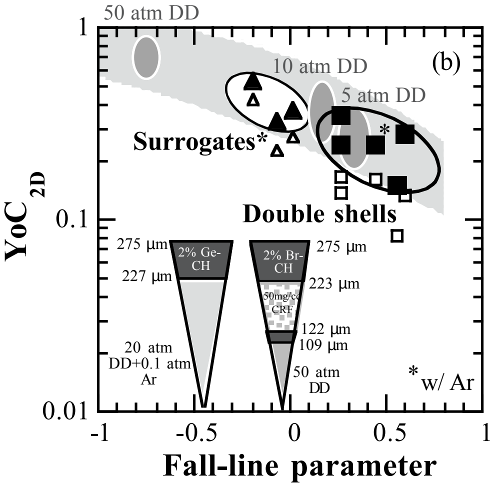

50 atm DD
10 atm DD
5 atm DD
(b)
Surrogates*
Double shells
*
*w/ Ar
275 µm
2% Ge-CH
227 µm
20 atm DD+0.1 atm Ar
2% Br-CH
275 µm
223 µm
50mg/cc CRF
122 µm
109 µm
50 atm DD
1
0.1
0.01
YoC$_{2D}$
-1
-0.5
0
0.5
1
Fall-line parameter

Fig. 6

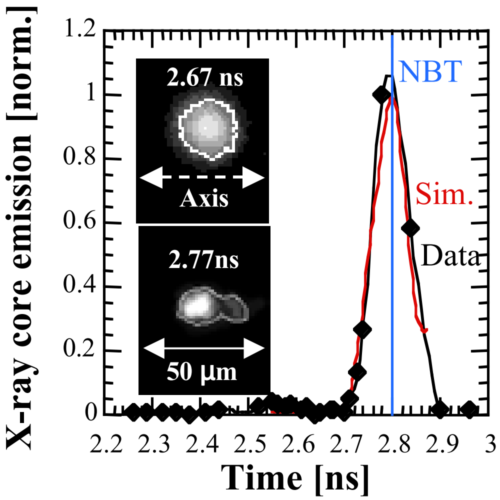

2.67 ns
Axis
2.77ns
50 µm
NBT
Sim.
Data
1.2
1
0.8
0.6
0.4
0.2
0
2.2
2.3
2.4
2.5
2.6
2.7
2.8
2.9
3
X-ray core emission [norm.]
Time [ns]

Fig. 6

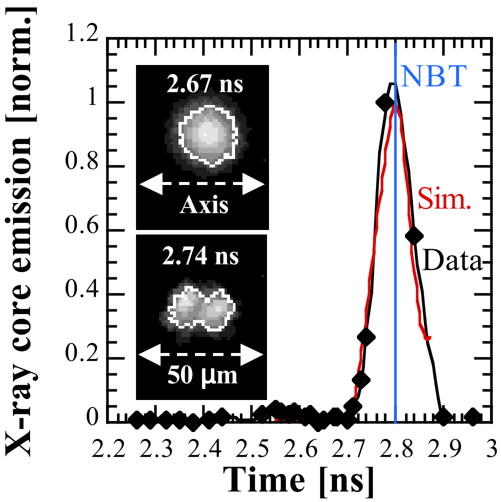
X-ray core emission [norm.]
1.2
1
0.8
0.6
0.4
0.2
0
2.2
2.3
2.4
2.5
2.6
2.7
2.8
2.9
3
Time [ns]
2.67 ns
Axis
2.74 ns
50 µm
NBT
Sim.
Data